Structural Basis for Cell Cycle Checkpoint Control by the BRCA1−CtIP Complex[†,‡]

Ashok K. Varma, Raymond S. Brown, Gabriel Birrane, and John A. A. Ladias*

Molecular Medicine Laboratory and Macromolecular Crystallography Unit, Division of Experimental Medicine, Harvard Institutes of Medicine, Harvard Medical School, Boston, Massachusetts 02115

Received May 24, 2005; Revised Manuscript Received July 13, 2005

ABSTRACT: The breast and ovarian tumor suppressor BRCA1 has important functions in cell cycle checkpoint control and DNA repair. Two tandem BRCA1 C-terminal (BRCT) domains are essential for the tumor suppression activity of BRCA1 and interact in a phosphorylation-dependent manner with proteins involved in DNA damage-induced checkpoint control, including the DNA helicase BACH1 and the CtBP-interacting protein (CtIP). The crystal structure of the BRCA1 BRCT repeats bound to the PTRVSpSPVF-GAT phosphopeptide corresponding to residues 322−333 of human CtIP was determined at 2.5 Å resolution. The peptide binds to a cleft formed by the interface of the two BRCTs in a two-pronged manner, with phospho-Ser327 and Phe330 anchoring the peptide through extensive contacts with BRCA1 residues. Several hydrogen bonds and salt bridges that stabilize the BRCA1−BACH1 complex are missing in the BRCA1−CtIP interaction, offering a structural basis for the ∼5-fold lower affinity of BRCA1 for CtIP compared to that of BACH1, as determined by isothermal titration calorimetry. Importantly, the side chain of Arg1775 in the cancer-associated BRCA1 mutation M1775R sterically clashes with the phenyl ring of CtIP Phe330, disrupting the BRCA1−CtIP interaction. These results provide new insights into the molecular mechanisms underlying the dynamic selection of target proteins involved in DNA repair and cell cycle control by BRCA1 and reveal how certain cancer-associated mutations affect these interactions.

The breast and ovarian cancer susceptibility gene 1 (*BRCA1*)[1] encodes a 1863-residue multifunctional protein that participates in genomic stability maintenance through its function in the repair of double-strand DNA breaks (DSBs), cell cycle checkpoint control, protein ubiquitination, and transcriptional regulation (*1*−*3*). *BRCA1* functions as a tumor suppressor, and germline mutations in this gene are associated with a high incidence of familial breast and ovarian cancer (*1*, *2*). The BRCA1 protein contains two BRCT domains that are frequent targets of cancer-causing mutations. In fact, the majority of clinically validated *BRCA1* mutations produce truncated BRCA1 polypeptides that lack one or both BRCT repeats, and several missense mutations that affect the structure of these domains are associated with early-onset breast and ovarian cancer (*2*, *4*). These findings, together with the observation that genetic deletion of the BRCA1 BRCT domains leads to tumor development in mice (*5*), demonstrate that the structural integrity of these modules is essential for the tumor suppressor activity of BRCA1.

Although the mechanisms underlying tumor suppression by BRCA1 remain largely unknown, mounting evidence indicates that the interaction of the BRCT domains with proteins involved in DNA damage-induced cell cycle checkpoint control and DNA repair plays a key role in this function (*1*−*3*). In response to genotoxic insults, such as ionizing radiation, BRCA1 is phosphorylated by the ATM kinase and localizes at DNA damage sites, where it is thought to participate in the assembly of DNA repair complexes. BRCA1 is an essential component of the DNA damage-induced S phase and G2/M phase checkpoints (*6*), and BRCA1-deficient cells exhibit defects in homology-directed DNA repair, being hypersensitive to ionizing radiation and agents that cross-link DNA strands or produce DSBs, such as cisplatin and mitomycin C (*7*−*10*). BRCA1 BRCT binding to the DNA helicase BACH1 (*11*) and the transcriptional corepressor CtIP (*12*−*14*) plays a central role in the G2/M checkpoint control (*15*, *16*). Recent studies have demonstrated that the BRCA1 BRCT repeats are phosphoprotein-binding modules (*17*−*19*) and have shown that phosphorylation of the BACH1 and CtIP proteins at Ser990 and Ser327, respectively, is essential for recognition by these domains (*16*, *18*, *19*). CtIP was originally identified as a binding partner of the transcriptional corepressor CtBP (*12*), and was subsequently shown to interact with and mediate transcriptional repression by the retinoblastoma (pRB) tumor suppressor and the pRB-related protein p130 (*20*). Importantly,

[†] This work was supported by Grants GM065520, DK062162, and AG021964 from the National Institutes of Health, DAMD170210300 and DAMD170310563 from the Department of Defense, an Experienced Investigator Award from the Massachusetts Department of Public Health, and Temple Discovery Award TLL035927 from the Alzheimer's Association to J.A.A.L.

[‡] The atomic coordinates and structure factors have been deposited in the Protein Data Bank as entry 1Y98.

* To whom correspondence should be addressed: Harvard Institutes of Medicine, 4 Blackfan Circle, Boston, MA 02115. Telephone: (617) 667-0064. Fax: (617) 975-5241. E-mail: jladias@bidmc.harvard.edu.

[1] Abbreviations: BACH1, BRCA1-associated C-terminal helicase; BRCA1, product of breast and ovarian cancer susceptibility gene 1; BRCT, BRCA1 C-terminal; CtIP, CtBP-interacting protein.

10.1021/bi0509651 CCC: $30.25
Published on Web 07/29/2005

CtIP is phosphorylated on Ser327 only in G2 phase and controls the G2/M transition checkpoint through its transient interaction with the BRCA1 BRCT repeats, which differs from the more stable BRCA1−BACH1 association that persists in the S through M phase and controls the G2 accumulation checkpoint (*16*, *18*, *19*).

Recently determined crystal and solution structures of the BRCA1 BRCT domains bound to BACH1 and artificial phosphopeptides have offered mechanistic insights into ligand recognition by these modules (*21*−*24*). The BACH1 peptide inserts in a conserved surface cleft at the junction of the two BRCT domains, with phospho-Ser990 and Phe993 of BACH1 providing the main interactions with BRCA1 residues. To further elucidate the specificity and affinity determinants of BRCT−ligand interactions, we determined the crystal structure of the BRCA1 BRCT repeats bound to a CtIP phosphopeptide. As in the BRCA1−BACH1 structures (*21*, *22*), CtIP phospho-Ser327 and Phe330 anchor the peptide to the conserved BRCT cleft. However, several hydrogen bonds and salt bridges that stabilize the BRCA1−BACH1 interaction are missing in the BRCA1−CtIP complex, providing a structural explanation for the lower affinity and transient nature of the association of BRCA1 with CtIP as compared to BACH1.

EXPERIMENTAL PROCEDURES

Protein Purification and Crystallization. The human BRCA1 BRCT protein (residues 1646−1859) was expressed in *Escherichia coli* BL21(DE3) cells as a glutathione *S*-transferase fusion, purified on glutathione−Sepharose, released with thrombin digestion, and further purified on a Superdex 75 column (Amersham Biosciences). The BRCT protein [25 mg/mL in phosphate-buffered saline (pH 7.4) supplemented with 300 mM NaCl] was mixed with the synthetic phosphopeptide PTRVSpSPVFGAT (pS denoting phosphoserine) at a 1:1.5 molar ratio and was crystallized by the sitting drop vapor diffusion method at 20 °C with addition of 1.75 M ammonium sulfate, 0.1 M MES (pH 6.7), and 10 mM cobalt chloride. Crystals were cryoprotected in mother liquor containing 25% glycerol and were flash-frozen in liquid nitrogen. Diffraction data were collected on beamline X12B at the National Synchrotron Light Source (Brookhaven National Laboratory, Long Island, NY). The crystals belong to space group $P6_122$ with the following unit cell dimensions: $a = b = 113.1$ Å, $c = 121.9$ Å, $\alpha = \beta = 90°$, and $\gamma = 120°$. The data were reduced and merged using DENZO and SCALEPACK (*25*) (Table 1).

Structure Determination and Refinement. The BRCT−CtIP structure was determined by molecular replacement using PHASER (*26*) and the BRCA1 BRCT−BACH1 structure (PDB entry 1T15) with the BACH1 peptide removed, as the search model. Refinement with CCP4 (*27*) and REFMAC5 (*28*) produced initial $2F_o - F_c$ and $F_o - F_c$ maps with continuous electron density for the CtIP peptide. The molecular geometry of the structure was improved with CNS (*29*) and by manual model building using O (*30*). Water molecules were found with ARP/wARP (*31*). The final model contains 1786 protein atoms, 48 water molecules, one sulfate ion, and one cobalt ion. The crystallized BRCT protein includes the vector-derived GS residues at its N terminus.

Table 1: Structure Determination and Refinement Statistics

resolution range (Å)	20−2.5
no. of observed reflections	179377
no. of unique reflections	16294
completeness (%)[a]	99.1 (99.4)
redundancy[a]	11.0 (6.4)
R_{sym} (%)[b]	13.3 (37.2)
overall $\langle I/\sigma(I)\rangle$	17.5 (2.7)
R_{cryst} (%)[c]	23.4
R_{free} (%)[d]	26.9
Ramachandran plot	
most favored (%)	79.0
additionally allowed (%)	18.5
generously allowed (%)	2.6
disallowed (%)	0.0
bond lengths[e] (Å)	0.016
bond angles[e] (deg)	1.78

[a] Values in parentheses are for the highest-resolution shell (2.59−2.50 Å). [b] $R_{sym} = \sum|I - \langle I\rangle|/\sum(I)$, where I is the observed integrated intensity, $\langle I\rangle$ is the average integrated intensity obtained from multiple measurements, and the summation is over all observed reflections. [c] $R_{cryst} = \sum||F_{obs}| - k|F_{calc}||/\sum|F_{obs}|$, where F_{obs} and F_{calc} are the observed and calculated structure factors, respectively. [d] R_{free} is calculated as R_{cryst} using 6.25% of the reflections chosen randomly and omitted from the refinement calculations. [e] Bond lengths and angles are root-mean-square deviations from ideal values.

Isothermal Titration Calorimetry. Binding constants for interaction of the BRCA1 BRCT domains with the BACH1 and CtIP phosphopeptides were measured using a VP-ITC microcalorimeter (MicroCal). Briefly, 0.1323 mM BACH1 peptide ISRSTpSPTFNKQ and 0.2096 mM CtIP peptide PTRVSpSPVFGAT were titrated against a 0.0188 mM solution of BRCA1 BRCT protein in phosphate-buffered saline and 300 mM NaCl at 25 °C. Titration curves were analyzed using ORIGIN 5.0 (OriginLab). Protein and peptide concentrations were determined by quantitative amino acid analysis on an ABI 420A derivatizer/analyzer and an ABI 130A separation system (Applied Biosystems).

RESULTS AND DISCUSSION

CtIP Phosphopeptide Recognition by the BRCA1 BRCT Domains. As described previously (*21*−*24*), the BRCA1 region spanning residues 1646−1859 folds into two tandem domains (BRCT1 and BRCT2), each comprising a central β-sheet formed by four parallel β-strands ($\beta1-\beta4$) and flanked by two α-helices (α1 and α3) on one side and a single α-helix (α2) on the other (Figure 1). The two BRCT domains pack closely against each other in a head-to-tail manner, burying a large hydrophobic interface and creating a deep surface groove. The CtIP peptide binds to this groove in a two-pronged mode, with phospho-Ser327 (pSer 0) and Phe330 (Phe +3) forming the main interactions with the BRCT domains (Figures 1 and 2A,B), consistent with biochemical and functional studies on the importance of these residues for the association of BRCA1 with CtIP and other phosphopeptides (*16*−*19*). The phosphate group of pSer 0 forms hydrogen bonds with the side chains of BRCT1 residues Ser1655 and Lys1702, the amide nitrogen of Gly1656, and the amide nitrogen of Lys1702 through a water-mediated interaction (Figure 2A,C). The phenyl ring of Phe +3 is inserted into a hydrophobic pocket made up of residues Arg1699, Leu1701, Phe1704, Asn1774, Met1775, Arg1835, and Leu1839 from both BRCT1 and BRCT2 repeats, whereas the carbonyl oxygen and amide nitrogen

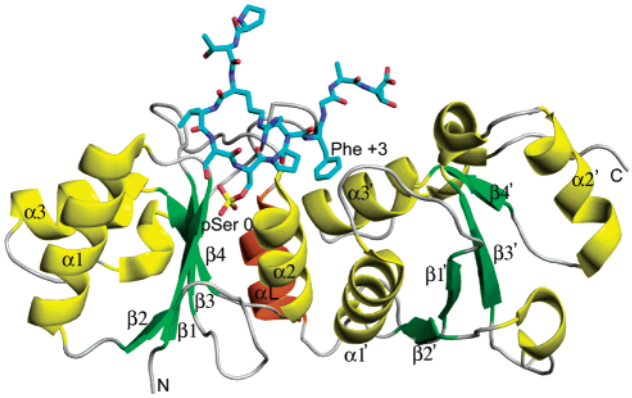

FIGURE 1: CtIP recognition by BRCA1 BRCT domains. Ribbon representation of the BRCA1 BRCTs bound to the CtIP peptide (cyan stick model). The α-helices and *β*-strands are colored yellow and green, respectively. The BRCT2 secondary structure elements are labeled with primes. BRCT linker helix αL is colored orange. Critical residues pSer 0 and Phe +3 are denoted. The figure was made using PyMOL (www.pymol.org) and POV-Ray (www.povray.org).

of Phe +3 hydrogen bond with N^{ϵ} and the carbonyl oxygen of Arg1699, respectively (Figure 2B,C). To a lesser degree, CtIP residues Val −2, Pro +1, and Gly +4 also contribute to the interaction though van der Waals contacts and water-mediated hydrogen bonds (Figure 2C).

Structural Basis for Disruption of the BRCA1−CtIP Interaction by Cancer-Associated Mutations. A number of missense mutations within the BRCT repeats abrogate the tumor suppression activity of BRCA1 and are associated with a high incidence of cancer, but there have been difficulties in explaining how they exert their effects. In two such mutations, M1775R and R1699W, the affected BRCT residues participate in the formation of the hydrophobic pocket that receives the Phe +3 phenyl ring of the BACH1 (*21*, *22*, *24*) and CtIP phosphopeptides (Figure 2B,C). The M1775R mutation inhibits the interaction of BRCA1 with BACH1 (*11*, *17*, *21*, *22*) and CtIP (*13*) and leads to defects in the DSB repair (*32*) and transactivation functions of BRCA1 (*33*). Superposition of the BRCA1−CtIP and unbound mutant BRCT(M1775R) crystal structures (*34*)

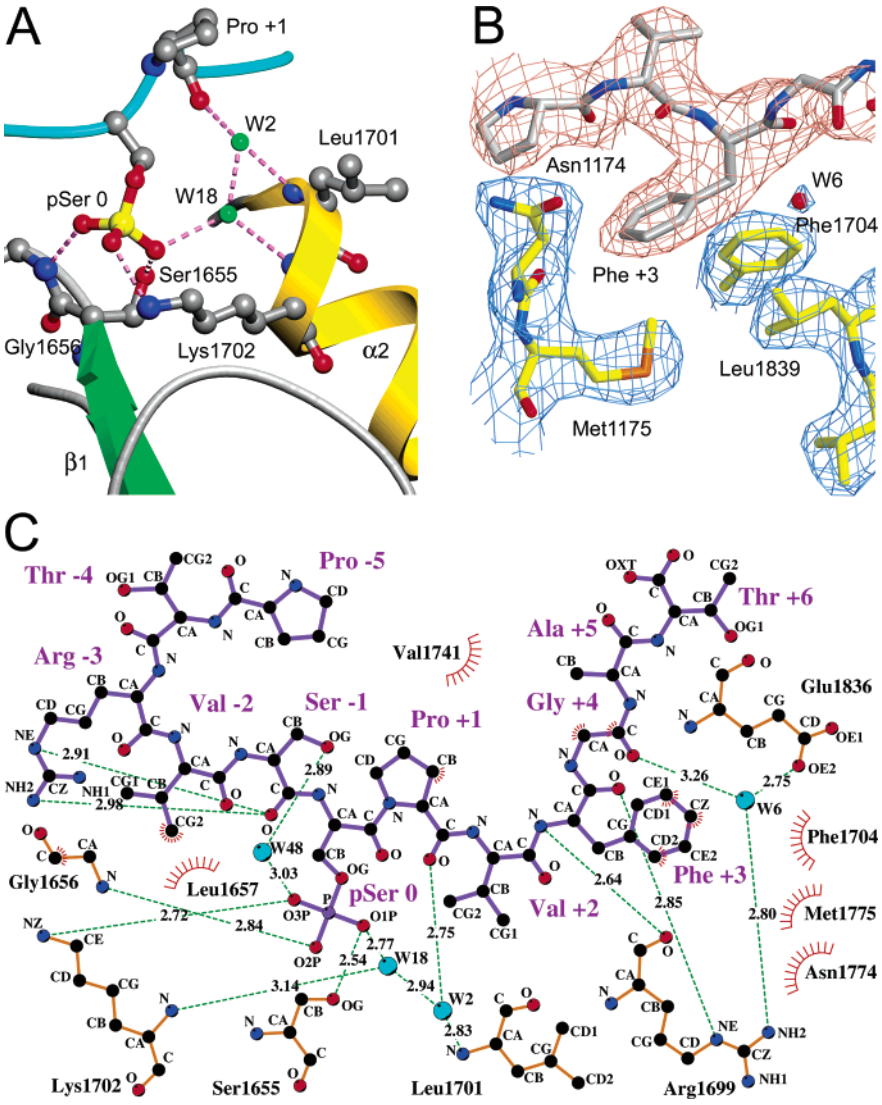

FIGURE 2: (A) Ribbon diagram of the CtIP pSer 0 interactions with residues in the BRCT1 repeat. Hydrogen bonds are represented as pink dashed lines and water molecules as green spheres. (B) A σ_A-weighted annealed omit map (beige) enveloping the CtIP peptide is superimposed on a σ_A-weighted $2F_o - F_c$ electron density map (blue) covering the BRCT residues at the Phe +3 binding site. The maps were calculated at 2.5 Å resolution and contoured at 1.0σ. This figure was made with BOBSCRIPT (*42*). (C) Two-dimensional representation of the interactions between BRCA1 (orange) and CtIP (purple) residues. Water molecules (W) are shown as cyan spheres, hydrogen bonds as dashed lines, and hydrophobic interactions as arcs with radial spokes. This figure was made using LIGPLOT (*43*).

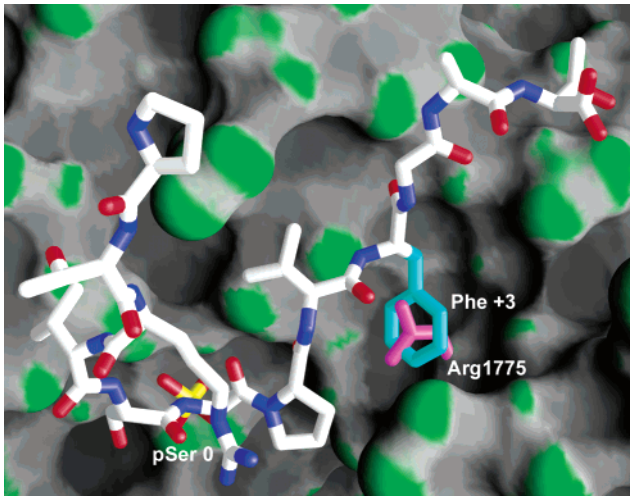

FIGURE 3: Occlusion of CtIP Phe +3 by the cancer-associated mutation M1775R. Superposition of the BRCT−CtIP and BRCT-(M1775R) mutant (PDB entry 1N5O) crystal structures shows the steric hindrance between the Arg1775 (pink) and Phe +3 (cyan) side chains. This figure was made with GRASP (*44*).

shows that the guanidino group of the substituted Arg1775 sterically clashes with the phenyl ring of Phe +3, directly obstructing the insertion of this anchoring group into the pocket (Figure 3), as described for the effect of M1775R on the BRCA1−BACH1 interaction (*21*−*24*). In the case of R1699W, it is predicted that the hydrogen bond between N^{ϵ} of Arg1699 and the carbonyl oxygen of Phe +3 will be lost and the large indole group of Trp1699 will likely occlude the entrance of the phenyl ring into the pocket.

Comparison of the BRCT−CtIP and BRCT−BACH1 Complexes. Superposition of the BRCA1−CtIP and BRCA1−BACH1 structures shows that the BRCT repeats and the backbones of five residues (pSer 0 to Gly +4) are superimposed well (root-mean-square deviation of 0.71 Å for all C^{α} atoms), whereas the N- and C-terminal portions of the peptides are not superimposable (Figure 4A). The O^{γ} atom of the BACH1 Ser −2 hydrogen bonds to the amide nitrogen of Gly1656, whereas in the BRCT−CtIP complex, the $C^{\gamma 2}$ atom of the Val −2 isopropyl group makes hydrophobic contacts with Leu1657 and displaces the peptide backbone away from the BRCT groove (Figure 2C). Interestingly, the guanidino group of CtIP Arg −3 folds back and forms two hydrogen bonds with the carbonyl oxygen of Ser −1, further stabilizing the peptide orientation and preventing any additional N-terminal interactions. Notably, a similar interaction of Arg −3 has not been observed in any of the BRCA1−BACH1 structures (*21*, *22*).

Additional differences in the interaction of the BRCTs with BACH1 and CtIP are observed at the C-terminal regions of the phosphopeptides. Whereas the side chain of BACH1 Asn +4 makes two water-mediated hydrogen bonds with BRCT residues Glu1689 and Arg1699 (*22*), these bonds are missing in the BRCA1−CtIP structure because a glycine occupies position +4 in CtIP (Figure 2C). Likewise, the side chain of BACH1 Lys +5 makes salt bridges with Glu1863 and Asp1840 (*22*), while similar interactions are missing in the BRCA1−CtIP complex due to the presence of Ala +5 in CtIP. The fewer interactions observed in the association of the BRCA1 BRCT repeats with CtIP than for BACH1 suggest a weaker association of these domains with the former phosphopeptide.

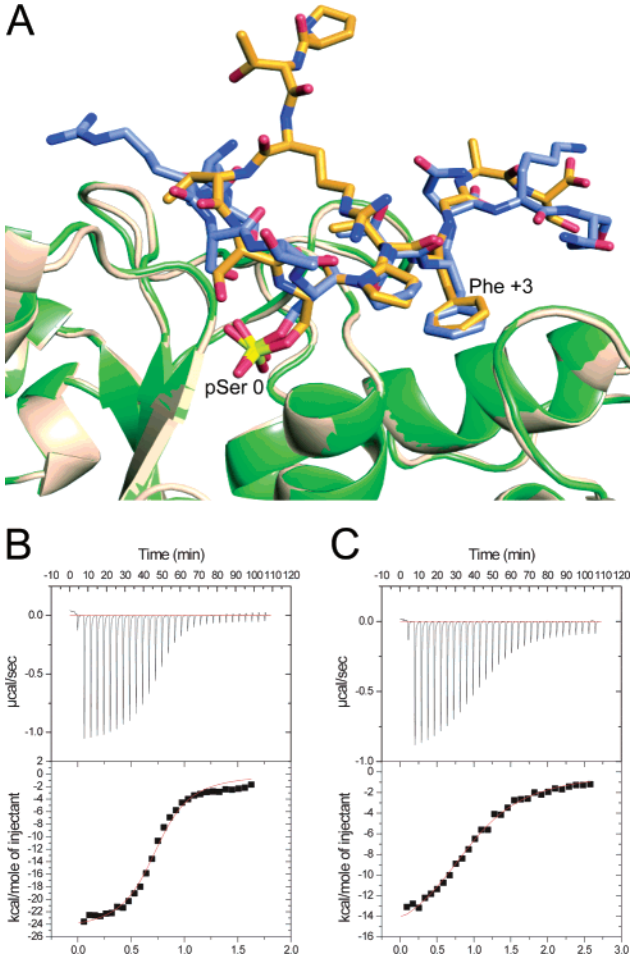

FIGURE 4: Comparison of the BRCA1−BACH1 and BRCA1−CtIP interactions. (A) Superposition of the crystal structures of the BRCA1 BRCTs (beige) bound to the BACH1 peptide (blue stick model) (PDB entry 1T29) and the BRCTs (green) bound to CtIP (orange stick model). (B and C) Representative isothermal titration calorimetry results obtained for the interaction of BRCA1 BRCT with the BACH1 and CtIP phosphopeptides, respectively.

The BRCA1 BRCT Domains Exhibit a Higher Affinity for BACH1 than CtIP. To determine the effects of these structural differences in the strength of the BRCA1−CtIP and BRCA1−BACH1 interactions, we measured the affinities of these complexes using isothermal titration calorimetry. The BRCA1 BRCT domains bind to the BACH1 phosphopeptide with a dissociation constant (K_d) of 0.7 μM (Figure 4B), which is in good agreement with the reported K_d of 0.9 μM for a similar BACH1 peptide (*21*). By contrast, the BRCT repeats bind to the CtIP phosphopeptide with a K_d of 3.7 μM (Figure 4C). The ∼5-fold higher binding affinity of the BRCA1 BRCTs for BACH1 than for CtIP can be attributed mainly to the hydrogen bonding network involving BACH1 residues Ser −2, Asn +4, and Lys +5 that is missing in the BRCA1−CtIP complex. These findings support the conclusion that residues surrounding pSer 0 and Phe +3 make significant contributions to the BRCT−ligand interaction and account for the affinity differences of various binding partners for the BRCT modules. These differences determine both the dynamic target selection among competing proteins that have distinct roles in cell cycle checkpoints and DNA repair for binding to BRCA1 and the duration of these interactions. For example, the association of the BRCA1 BRCT repeats with BACH1 leads to a stable

complex that accumulates in the G2 and M phases of the cell cycle, whereas the lower affinity of these domains for CtIP generates a transient complex during the G2 phase that controls the G2/M transition checkpoint (*16*).

Structural and Functional Implications. In addition to BACH1 and CtIP, other potential binding targets for the BRCA1 BRCT repeats have been identified in database searches with their consensus binding motif (*19*), including BRCA1 itself, the DNA mismatch repair protein MSH3 (*35*), hTID1, the human homologue of the *Drosophila* tumor suppressor l(2)Tid that modulates apoptosis (*36*), the CCCTC-binding factor CTCF that functions as a chromatin insulator and transcription factor implicated in the regulation of *BRCA1* gene expression (*37*), and the nuclear receptor co-activator NCoA-3/AIB1 that is amplified in breast and ovarian cancer (*38*) and regulates the estrogen-mediated survival and proliferation of breast carcinoma cells (*39*). Structural and biophysical analyses of the BRCA1 BRCT domains bound to their targets, including CtIP, BACH1, and the aforementioned proteins, will elucidate the mechanisms underlying the dynamic interactions of these versatile modules with various proteins during cell cycle control, DNA repair, chromatin remodeling, and transcription regulation. Furthermore, these studies will provide a structural explanation for the detrimental effects of breast and ovarian cancer-linked BRCT missense mutations on BRCA1 function.

Importantly, the atomic structures of the BRCA1 BRCT domains bound to CtIP, BACH1, and other targets could be exploited in improving current radiation therapy protocols for cancer. Because DNA damage-induced cell cycle checkpoints confer radioresistance to tumor cells, it has been suggested that inhibition of the checkpoint and DNA repair processes could result in more effective cancer treatments (*40*). BRCA1 controls the G2/M checkpoint through interactions with BACH1 and CtIP (*16*) and induces a large increase in resistance to agents that generate DSBs (*41*), whereas BRCA1-deficient cells are hypersensitive to ionizing radiation and DNA cross-linking agents (*9*, *10*, *32*). It is therefore conceivable that the atomic models of the BRCA1 BRCT domains bound to CtIP, BACH1, and other targets could provide a structural framework for the design of small-molecule inhibitors of these interactions that would enhance the sensitivity of tumor cells to radiation therapy and chemotherapy.

ACKNOWLEDGMENT

We thank the staff at the National Synchrotron Light Source for assistance during data collection and Dr. Donald Coen at Harvard Medical School for providing access to the microcalorimeter facility.

REFERENCES

1. Narod, S. A., and Foulkes, W. D. (2004) BRCA1 and BRCA2: 1994 and beyond, *Nat. Rev. Cancer 4*, 665−676.
2. Rosen, E. M., Fan, S., Pestell, R. G., and Goldberg, I. D. (2003) BRCA1 gene in breast cancer, *J. Cell. Physiol. 196*, 19−41.
3. Sancar, A., Lindsey-Boltz, L. A., Unsal-Kacmaz, K., and Linn, S. (2004) Molecular mechanisms of mammalian DNA repair and the DNA damage checkpoints, *Annu. Rev. Biochem. 73*, 39−85.
4. Vallon-Christersson, J., Cayanan, C., Haraldsson, K., Loman, N., Bergthorsson, J. T., Brondum-Nielsen, K., Gerdes, A. M., Moller, P., Kristoffersson, U., Olsson, H., Borg, A., and Monteiro, A. N. (2001) Functional analysis of BRCA1 C-terminal missense mutations identified in breast and ovarian cancer families, *Hum. Mol. Genet. 10*, 353−360.
5. Ludwig, T., Fisher, P., Ganesan, S., and Efstratiadis, A. (2001) Tumorigenesis in mice carrying a truncating Brca1 mutation, *Genes Dev. 15*, 1188−1193.
6. Xu, B., Kim, S., and Kastan, M. B. (2001) Involvement of Brca1 in S-phase and G_2-phase checkpoints after ionizing irradiation, *Mol. Cell. Biol. 21*, 3445−3450.
7. Moynahan, M. E., Chiu, J. W., Koller, B. H., and Jasin, M. (1999) Brca1 controls homology-directed DNA repair, *Mol. Cell 4*, 511−518.
8. Xu, X., Weaver, Z., Linke, S. P., Li, C., Gotay, J., Wang, X. W., Harris, C. C., Ried, T., and Deng, C. X. (1999) Centrosome amplification and a defective G_2-M cell cycle checkpoint induce genetic instability in BRCA1 exon 11 isoform-deficient cells, *Mol. Cell 3*, 389−395.
9. Bhattacharyya, A., Ear, U. S., Koller, B. H., Weichselbaum, R. R., and Bishop, D. K. (2000) The breast cancer susceptibility gene BRCA1 is required for subnuclear assembly of Rad51 and survival following treatment with the DNA cross-linking agent cisplatin, *J. Biol. Chem. 275*, 23899−23903.
10. Moynahan, M. E., Cui, T. Y., and Jasin, M. (2001) Homology-directed DNA repair, mitomycin-C resistance, and chromosome stability is restored with correction of a Brca1 mutation, *Cancer Res. 61*, 4842−4850.
11. Cantor, S. B., Bell, D. W., Ganesan, S., Kass, E. M., Drapkin, R., Grossman, S., Wahrer, D. C., Sgroi, D. C., Lane, W. S., Haber, D. A., and Livingston, D. M. (2001) BACH1, a novel helicase-like protein, interacts directly with BRCA1 and contributes to its DNA repair function, *Cell 105*, 149−160.
12. Schaeper, U., Subramanian, T., Lim, L., Boyd, J. M., and Chinnadurai, G. (1998) Interaction between a cellular protein that binds to the C-terminal region of adenovirus E1A (CtBP) and a novel cellular protein is disrupted by E1A through a conserved PLDLS motif, *J. Biol. Chem. 273*, 8549−8552.
13. Yu, X., Wu, L. C., Bowcock, A. M., Aronheim, A., and Baer, R. (1998) The C-terminal (BRCT) domains of BRCA1 interact in vivo with CtIP, a protein implicated in the CtBP pathway of transcriptional repression, *J. Biol. Chem. 273*, 25388−25392.
14. Wong, A. K., Ormonde, P. A., Pero, R., Chen, Y., Lian, L., Salada, G., Berry, S., Lawrence, Q., Dayananth, P., Ha, P., Tavtigian, S. V., Teng, D. H., and Bartel, P. L. (1998) Characterization of a carboxy-terminal BRCA1 interacting protein, *Oncogene 17*, 2279−2285.
15. Yu, X., and Baer, R. (2000) Nuclear localization and cell cycle-specific expression of CtIP, a protein that associates with the BRCA1 tumor suppressor, *J. Biol. Chem. 275*, 18541−18549.
16. Yu, X., and Chen, J. (2004) DNA damage-induced cell cycle checkpoint control requires CtIP, a phosphorylation-dependent binding partner of BRCA1 C-terminal domains, *Mol. Cell. Biol. 24*, 9478−9486.
17. Manke, I. A., Lowery, D. M., Nguyen, A., and Yaffe, M. B. (2003) BRCT repeats as phosphopeptide-binding modules involved in protein targeting, *Science 302*, 636−639.
18. Yu, X., Chini, C. C., He, M., Mer, G., and Chen, J. (2003) The BRCT domain is a phospho-protein binding domain, *Science 302*, 639−642.
19. Rodriguez, M., Yu, X., Chen, J., and Songyang, Z. (2003) Phosphopeptide binding specificities of BRCA1 COOH-terminal (BRCT) domains, *J. Biol. Chem. 278*, 52914−52918.
20. Meloni, A. R., Smith, E. J., and Nevins, J. R. (1999) A mechanism for Rb/p130-mediated transcription repression involving recruitment of the CtBP corepressor, *Proc. Natl. Acad. Sci. U.S.A. 96*, 9574−9579.
21. Shiozaki, E. N., Gu, L., Yan, N., and Shi, Y. (2004) Structure of the BRCT repeats of BRCA1 bound to a BACH1 phosphopeptide: Implications for signaling, *Mol. Cell 14*, 405−412.
22. Clapperton, J. A., Manke, I. A., Lowery, D. M., Ho, T., Haire, L. F., Yaffe, M. B., and Smerdon, S. J. (2004) Structure and mechanism of BRCA1 BRCT domain recognition of phosphorylated BACH1 with implications for cancer, *Nat. Struct. Mol. Biol. 11*, 512−518.
23. Williams, R. S., Lee, M. S., Hau, D. D., and Glover, J. N. (2004) Structural basis of phosphopeptide recognition by the BRCT domain of BRCA1, *Nat. Struct. Mol. Biol. 11*, 519−525.
24. Botuyan, M. V., Nomine, Y., Yu, X., Juranic, N., Macura, S., Chen, J., and Mer, G. (2004) Structural basis of BACH1 phosphopeptide recognition by BRCA1 tandem BRCT domains, *Structure 12*, 1137−1146.

25. Otwinowski, Z., and Minor, W. (1997) Processing of X-ray diffraction data collected in oscillation mode, *Methods Enzymol. 276*, 307−326.
26. Storoni, L. C., McCoy, A. J., and Read, R. J. (2004) Likelihood-enhanced fast rotation functions, *Acta Crystallogr. D60*, 432−438.
27. Collaborative Computational Project, Number 4 (1994) The CCP4 Suite: Programs for Protein Crystallography, *Acta Crystallogr. D50*, 760−763.
28. Murshudov, G. N., Vagin, A. A., and Dodson, E. J. (1997) Refinement of macromolecular structures by the maximum-likelihood method, *Acta Crystallogr. D53*, 240−255.
29. Brunger, A. T., Adams, P. D., Clore, G. M., DeLano, W. L., Gros, P., Grosse-Kunstleve, R. W., Jiang, J. S., Kuszewski, J., Nilges, M., Pannu, N. S., Read, R. J., Rice, L. M., Simonson, T., and Warren, G. L. (1998) Crystallography & NMR system: A new software suite for macromolecular structure determination, *Acta Crystallogr. D54*, 905−921.
30. Jones, T. A., Zou, J. Y., Cowan, S., and Kjeldgaard, M. (1991) Improved methods for building protein models in electron density maps and the location of errors in these models, *Acta Crystallogr. A47*, 110−119.
31. Perrakis, A., Morris, R., and Lamzin, V. S. (1999) Automated protein model building combined with iterative structure refinement, *Nat. Struct. Biol. 6*, 458−463.
32. Scully, R., Ganesan, S., Vlasakova, K., Chen, J., Socolovsky, M., and Livingston, D. M. (1999) Genetic analysis of BRCA1 function in a defined tumor cell line, *Mol. Cell 4*, 1093−1099.
33. Monteiro, A. N., August, A., and Hanafusa, H. (1996) Evidence for a transcriptional activation function of BRCA1 C-terminal region, *Proc. Natl. Acad. Sci. U.S.A. 93*, 13595−13599.
34. Williams, R. S., and Glover, J. N. (2003) Structural consequences of a cancer-causing BRCA1-BRCT missense mutation, *J. Biol. Chem. 278*, 2630−2635.
35. Kleczkowska, H. E., Marra, G., Lettieri, T., and Jiricny, J. (2001) hMSH3 and hMSH6 interact with PCNA and colocalize with it to replication foci, *Genes Dev. 15*, 724−736.
36. Syken, J., De-Medina, T., and Munger, K. (1999) TID1, a human homolog of the *Drosophila* tumor suppressor l(2)tid, encodes two mitochondrial modulators of apoptosis with opposing functions, *Proc. Natl. Acad. Sci. U.S.A. 96*, 8499−8504.
37. Butcher, D. T., Mancini-DiNardo, D. N., Archer, T. K., and Rodenhiser, D. I. (2004) DNA binding sites for putative methylation boundaries in the unmethylated region of the BRCA1 promoter, *Int. J. Cancer 111*, 669−678.
38. Anzick, S. L., Kononen, J., Walker, R. L., Azorsa, D. O., Tanner, M. M., Guan, X. Y., Sauter, G., Kallioniemi, O. P., Trent, J. M., and Meltzer, P. S. (1997) AIB1, a steroid receptor coactivator amplified in breast and ovarian cancer, *Science 277*, 965−968.
39. Weldon, C. B., Elliott, S., Zhu, Y., Clayton, J. L., Curiel, T. J., Jaffe, B. M., and Burow, M. E. (2004) Regulation of estrogen-mediated cell survival and proliferation by p160 coactivators, *Surgery 136*, 346−354.
40. Hartwell, L. H., and Kastan, M. B. (1994) Cell cycle control and cancer, *Science 266*, 1821−1828.
41. Quinn, J. E., Kennedy, R. D., Mullan, P. B., Gilmore, P. M., Carty, M., Johnston, P. G., and Harkin, D. P. (2003) BRCA1 functions as a differential modulator of chemotherapy-induced apoptosis, *Cancer Res. 63*, 6221−6228.
42. Esnouf, R. M. (1997) An extensively modified version of MolScript that includes greatly enhanced coloring capabilities, *J. Mol. Graphics Modell. 15*, 132−134.
43. Wallace, A. C., Laskowski, R. A., and Thornton, J. M. (1995) Derivation of 3D coordinate templates for searching structural databases: Application to Ser-His-Asp catalytic triads in the serine proteinases and lipases, *Protein Eng. 8*, 127−134.
44. Nicholls, A., Sharp, K. A., and Honig, B. (1991) Protein folding and association: Insights from the interfacial and thermodynamic properties of hydrocarbons, *Proteins 11*, 281−296.

BI0509651